The Photophysical Properties of the Adenine Chromophore

Joakim Andréasson, Anders Holmén,† and Bo Albinsson*

Department of Physical Chemistry, Chalmers University of Technology, SE−412 96 Göteborg, Sweden

Received: June 9, 1999; In Final Form: August 26, 1999

The efficient nonradiative deactivation process of the excited adenine chromophore is studied in this paper. By comparing the photophysical properties and temperature dependence of several alkylated adenine derivatives, a mechanism for the thermally activated internal conversion process is suggested. Several alkylamino derivatives of adenine show dual fluorescence, and the solvent dependence of the excited states is investigated. It is concluded that the long wavelength emission originates from a CT state involving the alkylamino group and purine chromophore as donor and acceptor, respectively. The experimental observations are supported by quantum mechanical calculations, and the results are summarized into a model for the photophysical properties of the adenine chromophore. In this model, the two excited states associated with the dual emission from the alkylamino derivatives are populated from a common Franck−Condon state followed by independent decay to the ground state.

Introduction

The normal nucleic acid bases (adenine, guanine, cytosine, thymine, and uracil) are nonfluorescent at room temperature.[1−4] Despite the difference in chemical composition and functionality, all of the nucleic acid bases have their lowest electronic absorption band around 260 nm. This gives a lowest singlet excited electronic state energy of about 5 eV (38 000 cm^{-1}) in excess over the ground state, which is an ample amount of energy to potentially be stored in the heart of our genetic machinery. The strategy to avoid damaging photochemistry in the nucleic acids carrying the genetic information (i.e., DNA and RNA) seems to be related to a mechanism that shortens the singlet excited state lifetime and, correspondingly, lowers the fluorescence quantum yield of the light absorbing bases.[3] It is interesting to note that nonreproducing nucleic acids contain odd bases with quite different photophysical properties, e.g., the Y-base in the transfer RNA, $tRNA^{Phe}$.[5,6] The mechanism for limiting the excited state lifetime of the normal nucleic acid bases is still unknown, and it is of the utmost importance to further investigate and to ultimately understand the complex photophysics of the DNA bases.

Several groups have investigated the photophysics of the adenine chromophore.[1,2,7−14] It was early realized that adenine and the other bases could exist in many different tautomeric forms with potentially very different fluorescence quantum yields. Adenine has the possibility to exist in two prototropic tautomers (7H and 9H) as well as in several imino (H−N═C) forms. Wilson and Callis have shown that the room-temperature emission from the adenine base is dominated by the 7H tautomer.[15] The fluorescence quantum yield of the 9-substituted adenine (e.g., adenosine) is 1 order of magnitude weaker at room temperature, and it is therefore essential to have appropriate control of the ground state species when discussing the weak emission from adenine and the other bases. In room temperature aqueous solution, adenosine has a fluorescence quantum yield of about 5×10^{-5} and the lowest excited singlet state has a reported lifetime of only 1.5 ps.[2,13,16,17]

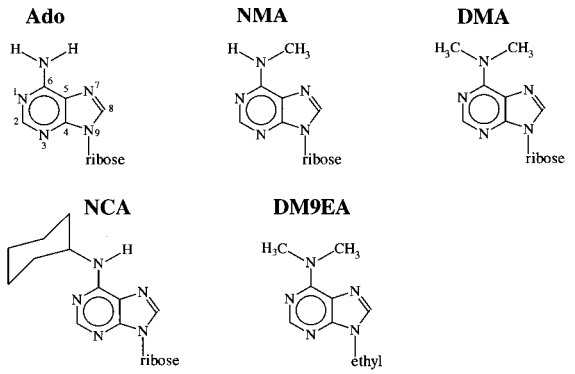

Figure 1. Adenine derivatives investigated: adenosine (Ado), N^6-methyladenosine, (NMA), N^6,N^6-dimethyladenosine (DMA), N^6-cyclohexyladenosine (NCA), and N^6,N^6-dimethyl-9-ethyladenine (DM9EA).

Recently, we observed that N^6,N^6-dimethyladenosine (DMA) showed dual fluorescence.[18] In addition to the normal weak short wavelength fluorescence at 330 nm (emission from an excited singlet state arbitrarily called the B-state), a long wavelength emission with peak maximum around 500 nm (emission from an excited singlet state arbitrarily called the A-state) was observed. The long wavelength emission was suggested to be due to an intramolecular excited state reaction forming the A-state which has significant charge transfer (CT) character. Tentatively we suggested the A-state to be a so-called twisted intramolecular charge transfer (TICT) state.[19−21] Furthermore, the complex kinetics and the temperature dependence of the radiationless processes suggested to us that the quenching of the primary excited state of DMA (the B-state) occurred via the A-state. Herbich and co-workers have made similar observations for different 4-(dialkylamino)pyrimidines and they interpret the dual emission from these compounds within the classical TICT framework.[22−25]

In this paper, we extend the study of photophysical properties to other alkylated adenine chromophores and in particular investigate the properties of the CT state. This is accomplished

* Corresponding author phone, 46-31-772 3044; fax, 46-31-772 3858; e-mail, balb@phc.chalmers.se

† Present address: Department of Substance Analysis, AstraZeneca Mölndal, SE−437 83 Mölndal, Sweden.

10.1021/jp991888k CCC: $18.00
Published on Web 10/07/1999

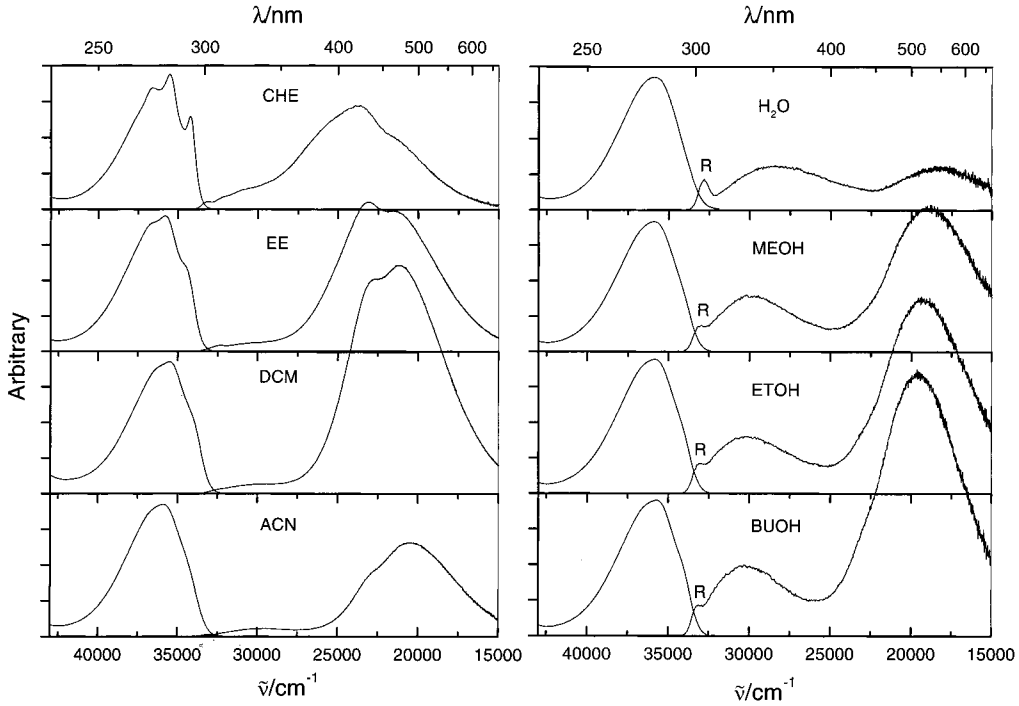

Figure 2. Absorption and fluorescence spectra of DM9EA in aprotic (left panel) and protic solvents (right panel). The spectra in each panel were measured on optically matched samples, and the intensity scales are therefore directly comparable. R denotes unavoidable Raman scattering from the solvents.

by a solvatochromic study in which the energy of the excited states of N^6,N^6-dimethyl-9-ethyladenine (DM9EA) are analyzed as a function of solvent polarity. The generality of our observation for adenine derivatives is demonstrated by including several differently substituted adenines (Figure 1), i.e., DMA, DM9EA, N^6-methyladenosine (NMA), N^6-cyclohexyladenosine (NCA), and adenosine (Ado). The relation between the formation of the A-state and nonradiative deactivation of the primary excited state for adenine derivatives is also thoroughly discussed.

Materials and Methods

Chemicals and Solvents. N^6,N^6-dimethyladenosine (DMA), N^6-methyladenosine (NMA), N^6-cyclohexyladenosine (NCA), and adenosine (Ado) were purchased from SIGMA and used without further purification. N^6,N^6-dimethyl-9-ethyladenine (DM9EA) and 9-methyladenine (9MA) were synthesized from N^6,N^6-dimethyladenine (from MERCK) and ethyliodide, and from adenine (MERCK) and methyliodide, respectively, by a procedure proposed by M. Hedayatullah[26] and purified by column chromatography on silica gel with chloroform/methanol/ammonia (90/15/1) as eluant. Acetonitrile (ACN), 1,2- dichloroethane (DCE), dichloromethane (DCM), 1,4-dioxane (DIOX), ethyl ether (EE), butanol (BUOH), and 2-methylbutane from MERCK; 2-methyltetrahydrufuran (MTHF) from ACROS; cyclohexane (CHE) from SIGMA; methanol (MEOH) from Lab-Scan; and ethanol (ETOH) from Kemetyl were all of spectroscopic grade. MTHF, dioxane, ethyl ether, dichloroethane, acetonitrile, and ethanol showed traces of fluorescent impurities and were distilled before use.

Spectroscopic Methods. Absorption spectra were recorded using a CARY 4B UV/vis spectrometer. Emission and excitation spectra were measured on a SPEX Fluorolog τ2 spectrofluorimeter. Quantum yields of fluorescence were determined by comparison with the emission spectrum of an optically matched sample of 2,5-diphenyl-1,3,4-oxadiazole (PPD) in cyclohexane ($\Phi_f = 0.89$).[27] The excitation spectra were recorded on dilute

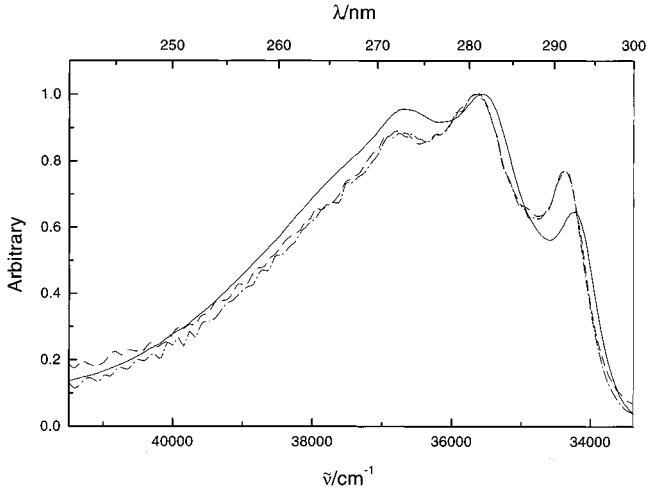

Figure 3. Comparison of the excitation (- - -, emission monitored at 330 nm; — · —, emission monitored at 500 nm) and absorption spectra (—) of DM9EA in cyclohexane.

samples (maximum absorbance below 0.1) to minimize inner filter effects. Fluorescence lifetimes were measured by using a time-correlated single-photon counting system. The samples were excited with a nitrogen filled flash lamp (Oxford instruments),[28] and a silica sol scatter solution was used as reference to record the lamp profile. The lamp profile was convoluted and the fluorescence decay was evaluated by multiexponential fitting using the Globals software.[29] The phosphorescence lifetime measurements were performed by manually closing the excitation shutter and recording the time dependent emission intensity. Low-temperature measurements were done in a liquid N_2-cooled cryostat (Oxford instruments DN 1704) with temperature regulator (DTC2).

Quantum chemical calculations were performed with the HyperChem[30] and Gaussian 94[31] programs. All ground state structures were fully optimized using the AM1, PM3, or MP2/

TABLE 1: Fluorescence and Absorption Properties for DM9EA in Different Solvents at Room Temperature[a]

solvent	ϵ	n	$\tilde{\nu}_{abs}$ /cm^{-1}	$\tilde{\nu}_{FB}$ /cm^{-1}	Φ_{FB}	$\tilde{\nu}_{FA}$ /cm^{-1}	Φ_{FA}	τ_{FA} /ns
ACN	37.50	1.342	35910	29880	1.7×10^{-4}	20370	3.2×10^{-3}	1.0
DCE	10.65	1.444	35520	30390	2.2×10^{-4}	21050	7.6×10^{-3}	1.6
DCM	9.08	1.424	35520	30460	1.8×10^{-4}	21210	9.2×10^{-3}	2.2
MTHF	6.97	1.404	35780	30640	1.6×10^{-4}	21550	6.7×10^{-3}	1.4
DIOX	2.21	1.420	35650	30680	2.0×10^{-4}	21250	7.9×10^{-3}	
EE	4.34	1.352	35780	31260	3.5×10^{-4}	21710	5.4×10^{-3}	1.1
CHE	2.02	1.426	35520	31480	1.3×10^{-4}	23840	4.7×10^{-3}	0.75
H_2O	78.54	1.333	35910	28070	2.0×10^{-4}	17960	1.8×10^{-4}	
MEOH	32.63	1.326	35910	29500	2.0×10^{-4}	18770	5.5×10^{-4}	
ETOH	24.55	1.361	35840	29680	2.2×10^{-4}	19100	7.6×10^{-4}	
BUOH	17.51	1.399	35650	29830	2.6×10^{-4}	19420	1.1×10^{-3}	

[a] The peak absorption wavenumber ($\tilde{\nu}_{abs}$), fluorescence maxima ($\tilde{\nu}_{FB}$, $\tilde{\nu}_{FA}$), and quantum yields (Φ_{FB}, Φ_{FA}) for the B- and A-fluorescence and the lifetime of the A-state (τ_{FA}) are listed.

6-31G* methods, and excited state properties were calculated with the INDO/S parameterization.

Results

The photophysical properties of the adenine chromophore are investigated in this paper. The material is organized as follows. First, the results from a solvatochromic study on DM9EA establish that the A-state has larger dipole moment than both the B-state and the ground state. This indicates that the A-state has substantial charge-transfer character. Second, the room temperature emissions from several adenine derivatives are compared, which gives further evidence for the CT character of the long wavelength emission. Finally, the thermal quenching of the short wavelength fluorescence is compared among the different adenine derivatives, and a tentative model for the photophysics of the adenine chromophore is proposed.

Dual Fluorescence from DM9EA. The absorption and fluorescence spectra of DM9EA in solvents with different polarities are shown in Figure 2. Dual fluorescence is observed at room temperature in all solvents studied, ranging from cyclohexane to water. The A-state fluorescence around 500 nm dominates in aprotic solvents but is quenched by protic solvents.[32] The B-state fluorescence at 330 nm has a low quantum yield ($\approx 10^{-4}$) in all solvents at room temperature. Table 1 comprises the room temperature spectroscopic characteristics for DM9EA. The position of the absorption maximum is approximately the same in all solvents (275 nm), but the positions of the two emission maxima depend on solvent polarity and it is clearly seen in Figure 2 and Table 1 that the A-state emission is substantially red-shifted as the solvent polarity increases.

Intramolecular Excited State Reaction. The two emission bands of DM9EA belong to the same ground state species as can be demonstrated by the fluorescence excitation spectra of DM9EA in cyclohexane shown in Figure 3. Monitoring either the B- or A-state emission band yields exactly the same band shape of the excitation spectra. The excitation spectra are also, within the experimental accuracy, superimposable on the absorption spectrum, showing that both emissions stem from a common UV absorber. In addition, the emission spectra of DM9EA in all studied solvents are independent of excitation wavelength. These observations strongly suggest that the A- and B-states are connected via an excited state reaction rather than being due to two different ground state species.

Dependence on Solvent Polarity. According to the theory of dielectric polarization,[33] the red shift of the fluorescence with increasing solvent polarity depends on the difference in permanent dipole moments of the ground and excited states. The magnitude of the excited state dipole moments can be estimated by the fluorescence solvatochromic shift method.[34−37] If the dipole moments are approximated by point dipoles in the center of a spherical cavity with radius a_0 and the mean solute polarizabilty is neglected, one obtains[35]

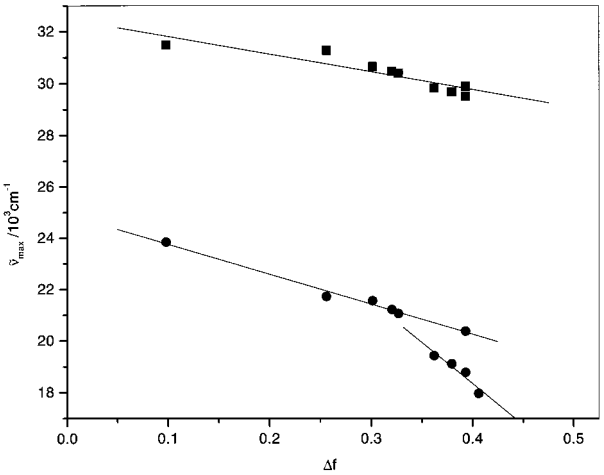

Figure 4. Position of the emission maxima for DM9EA in different solvents (● = A-fluorescence, ■ = B-fluorescence).

$$hc\tilde{\nu}_f = hc\tilde{\nu}_f^{vac} - \frac{2\boldsymbol{\mu}_e(\boldsymbol{\mu}_e - \boldsymbol{\mu}_g)}{a_0^3}\cdot\Delta f \qquad (1)$$

where $\tilde{\nu}_f$ and $\tilde{\nu}_f^{vac}$ are the spectral positions of the solvent equilibrated fluorescence maxima and the value extrapolated to gas-phase conditions, respectively; $\boldsymbol{\mu}_g$ and $\boldsymbol{\mu}_e$ are the dipole moments of the ground and excited states, and Δf is the Lippert solvent polarity parameter which describes the bulk solvent polarity

$$\Delta f = \frac{\epsilon - 1}{2\epsilon + 1} - \frac{1}{2}\frac{n^2 - 1}{2n^2 + 1} \qquad (2)$$

Here ϵ is the static dielectric constant and n is the refractive index of the solvent. In Figure 4, the spectral positions of the A- and B-state emissions from DM9EA are plotted against Δf. A linear relationship is found as predicted by eq 1 for the B-state emission including all solvents spanning from cyclohexane to water. For the A-state emission, the correlation is biphasic linear with one slope for the aprotic and another (larger) slope for the protic solvents. This might indicate specific interactions between DM9EA and proton donating solvents but could also reflect imperfections in the ability of the model to describe bulk solvent

TABLE 2: Magnitude and Orientation of the Ground State Permanent Dipole Moments for Adenine (Ade), N^6,N^6-Dimethyladenine (DMAde), N^6-Methyladenine (NMAde), 9-Ethyladenine (9EA), N^6,N^6-Dimethyl-9-ethyladenine (DM9EA), and N^6-Cyclohexyladenine (NCAde)

	$\|\mu\|$/D (α/deg)[a]				
	AM1	INDO/S//AM1	PM3	MP2/6-31G*	exp
Ade (9H)	2.18 (80°)	3.61 (95°)	2.19 (80°)		
DMAde (9H)	2.11 (80°)	3.37 (95°)	2.13 (80°)	2.33 (82°)	
NMAde (9H)	2.01 (80°)	3.61 (95°)	2.22 (oop)[b]		
9EA	2.60 (90°)	3.81 (95°)	3.02 (95°)		3.25 ± 0.2[c]
DM9EA	2.37 (90°)	3.56 (95°)	2.36 (90°)		
NCAde (9H)	1.80 (oop)[b]	3.67 (oop)[b]	1.95 (oop)[b]		

[a] Orientation of dipole moment; in-plane angle α relative to the C^4-C^5 bond counted positive clockwise. [b] The alkylamino group is twisted in the optimized ground state geometry giving an out-of-plane component to the dipole moment. [c] Experimental result for 9-methyladenine, ref 46.

TABLE 3: Experimental[a] and Calculated Excited State Dipole Moments for DM9EA and N^6,N^6-Dimethyladenine (9H)

		exp		INDO/S//AM1[b]		
		$\mu_e(\mu_e - \mu_g)$/D^2	$\|\mu_e\|$/D	$\mu_e(\mu_e - \mu_g)$/D^2	$\|\mu_e\|$/D	$\Delta\alpha$[c]/deg
DM9EA	B-state	51	7.4 ± 1.8	7.3	5.0	8
	A-state	88	9.5 ± 1.8	31	5.8	84
DMAde	B-state			6.1	4.7	8
	A-state			33	6.0	83

[a] The ground state dipole moment was estimated by an INDO/S// AM1 calculation (Table 2) and the Onsager radius ($a_0 = 4.2$ Å) was estimated by the mass−density approach.[47] [b] INDO/S-CI calculation for the AM1 optimized ground state geometry (representing the B-state) and for a similar structure with the dimethylamino group twisted 90° (representing the A-state). The CI consisted of all singly excited configurations from the 15 highest occupied molecular orbitals to the 15 lowest unoccupied (225 configurations). [c] Angle between ground and excited state dipole moment.

polarity.[38] If only the aprotic solvents are considered, the slope is about two times larger for the A-state compared to the B-state emission, which is consistent with a charge-transfer character of the A-state.

The excited state dipole moments for DM9EA are estimated from the slopes in Figure 4. Since the ground state dipole moment for DM9EA has not been determined experimentally, it was estimated by quantum mechanical calculations. The dipole moments for several adenine derivatives predicted by different computational methods are shown in Table 2. The magnitude of the calculated dipole moment depends on the methods used; the MNDO-based methods, AM1 and PM3, yield smaller dipole moments compared to the INDO/S parameterization. The AM1 and PM3 methods usually represent ground state electronic structure and geometries better compared to the INDO/S method, but since the excited states are expected to be more accurately described by the latter it is not obvious which method to prefer in this case. The experimentally determined dipole moment for 9-methyladenine is comparable in size to the calculated values, and a correlated ab initio calculation also yields results comparable to the semiempirical calculations (Table 2). We therefore believe the magnitude and directions of the ground state dipole moments to be accurately predicted by the computational methods.

The experimentally determined permanent excited state dipole moments are collected in Table 3 and compared to those estimated by INDO/S calculations. It is seen not only that experiments and theory agree in the relative trend ($\mu_A > \mu_B > \mu_g$) but also that the absolute values are quite different. Since the dipole moment is a vectorial property, the solvatochromic shift depends both on the change in dipole moment magnitude *and* direction according to eq 1. The dipole moments of the ground and B-states are predicted to be nearly parallel, and both are perpendicular to the dipole moment of the A-state. A large change in direction of the permanent dipole moments in the ground and excited states has a great influence on the solvatochromic shift (eq 1) and partly explains the difference in polarity dependence of the two emissions. The calculated directions of the ground state dipole moments are given in Table 2 for several adenine derivatives, and all calculations agree that the ground state dipole moment is oriented along the purine long axis. Now, if charge transfer from the dimethylamino group to the purine ring makes an important contribution, we would expect a short-axis oriented excited state dipole moment of the A-state. The results presented in Table 3 are consistent with this interpretation.

Time-Resolved Fluorescence. The two emissions have very different fluorescence lifetimes. At room temperature, the decay of the B-state fluorescence could not be separated from the exciting pulse, which indicates a lifetime of less than about 100 ps. The A-state is more long-lived with lifetimes in the region 1−2 ns in different aprotic solvents (Table 1). As will be shown in the next paragraph, the B-state fluorescence quantum yield is strongly dependent on temperature, whereas the A-state fluorescence quantum yield is almost temperature independent. Since the radiative rate constants usually are temperature independent, the increase in B-state fluorescence quantum yield is expected to be paralleled by a proportional increase in fluorescence lifetime. At 152 K in MTHF, the two emissions are of similar intensity and the B-state is expected to be sufficiently long-lived to be resolved by our flash-lamp system. Indeed, monitoring 9 different emission wavelengths in the region 330−600 nm and globally analyzing the decays yielded two lifetimes of 0.17 ns and 2.1 ns dominating the B- and A-state fluorescence, respectively. The fractional contribution from these decay times at the different emission wavelengths are shown in Figure 5 together with the steady-state fluorescence spectrum of DM9EA in MTHF at 152 K. The fitted parameters are compiled in Table 4.

Other N^6-Alkylated Adenine Derivatives. We have observed dual fluorescence from several N^6-alkylated adenine derivatives. In Figure 6, the emission spectra of DMA, NMA, NCA, and adenosine are compared and the spectral positions and quantum yields are collected in Table 5. The emission spectrum of DMA is very similar to the emission spectrum of DM9EA. This is expected since an ethyl or a ribose group as N^9 substituent is not expected to make a large difference. In NMA, the N^6-amino group is monoalkylated and this has a large effect on the A-state fluorescence while the B-state fluorescence is less affected showing clearly that the alkylated amino group is important for the properties of the A-state. Upon removal of one of the methyls from DMA the A-state emission blue-shifts about 4000 cm^{-1} and loses intensity. Both of these observations

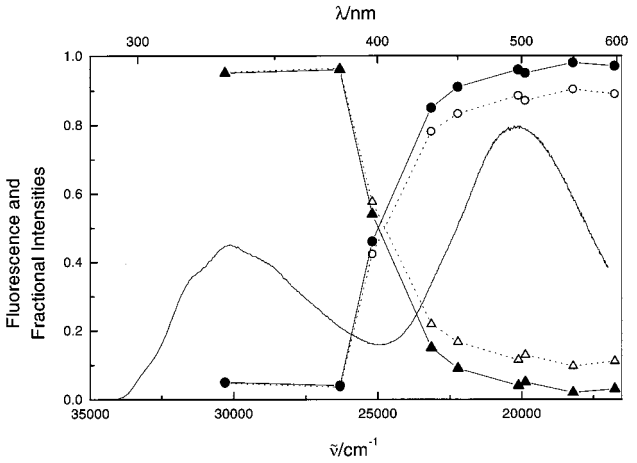

Figure 5. Fractional contribution to the biexponential decays compared to the steady-state emission spectra of DM9EA in MTHF at 152 K. The filled symbols show fractional intensities for two independent emitting species, and the unfilled symbols the fractional intensities for two excited state species interconnected by an irreversible reaction (cf. Table 4).

TABLE 4: Globally Analyzed Lifetimes[a], Preexponential Factors, and Fractional Intensities for DM9EA in MTHF at 152 K

$\tilde{\nu}$/cm^{-1}	α_1	τ_1/ns	f_1[b]	F_1[c]	α_2	τ_2/ns	f_2[b]	F_2[c]	χ^2
30 300	4.84	0.17	0.95	0.95	0.02	2.13	0.05	0.05	1.7
26 300	6.42	0.17	0.96	0.96	0.02	2.13	0.04	0.04	1.4
25 200	4.45	0.17	0.58	0.54	0.30	2.13	0.42	0.46	2.7
23 150	1.00	0.17	0.22	0.15	0.45	2.13	0.78	0.85	3.0
22 200	0.14	0.17	0.17	0.09	0.11	2.13	0.83	0.91	1.9
20 100	0.19	0.17	0.11	0.04	0.39	2.13	0.89	0.96	1.3
19 900	0.47	0.17	0.13	0.05	0.66	2.13	0.87	0.95	1.2
18 200	0.12	0.17	0.10	0.02	0.63	2.13	0.90	0.98	1.4
16 750	0.22	0.17	0.11	0.03	0.52	2.13	0.89	0.97	1.5

[a] The emission decays were fitted globally to a biexponential expression: $I(t,\lambda) = \alpha_1(\lambda)\exp(-t/\tau_1) + \alpha_2(\lambda)\exp(-t/\tau_2)$ where the two lifetimes (τ_1 and τ_2) were linked and the preexponential factors (α_1 and α_2) varied freely. [b] Fractional intensities calculated for an irreversible excited state reaction, 1→2:

$$f_1(\lambda) = \tau_2^{-1}\frac{\alpha_1(\lambda) + \alpha_2(\lambda)}{\alpha_1(\lambda)\tau_2^{-1} + \alpha_2(\lambda)\tau_1^{-1}} \quad f_2(\lambda) = \frac{\alpha_2(\lambda)(\tau_1^{-1} - \tau_2^{-1})}{\alpha_1(\lambda)\tau_2^{-1} + \alpha_2(\lambda)\tau_1^{-1}}$$

[c] Fractional intensities calculated for two independent excited species:

$$F_1(\lambda) = \frac{\alpha_1(\lambda)\tau_1}{\alpha_1(\lambda)\tau_1 + \alpha_2(\lambda)\tau_2} \quad F_2(\lambda) = \frac{\alpha_2(\lambda)\tau_2}{\alpha_1(\lambda)\tau_1 + \alpha_2(\lambda)\tau_2}$$

are consistent with a charge-transfer character of the A-state. The energy of a pure charge-transfer transition is a linear function of the ionization potential of the donor moiety.[39,40] The ionization potential increases by 0.4 eV when removing one methyl from dimethylethylamine ($(CH_3)_2NCH_2CH_3 \rightarrow CH_3NHCH_2CH_3$)[41] which corresponds to a blue-shift of about 3200 cm^{-1}. Although the simple aliphatic amines are not directly comparable to our systems, the fact that the observed spectral shift has the same magnitude as that expected from the change in ionization potential strongly advocates the charge-transfer assignment.

In addition to the spectral shift, the intensity of the A-state fluorescence is much lower for NMA compared to DMA (Figure 6, Table 5). If the A-state is formed from the B-state in an excited state reaction, it is expected that the rate constant for the formation of the A-state decreases as a consequence of the destabilization. As the energy of the A-state increases with the B-state energy nearly unchanged, the barrier separating the two states is expected to increase, and the observed decrease in

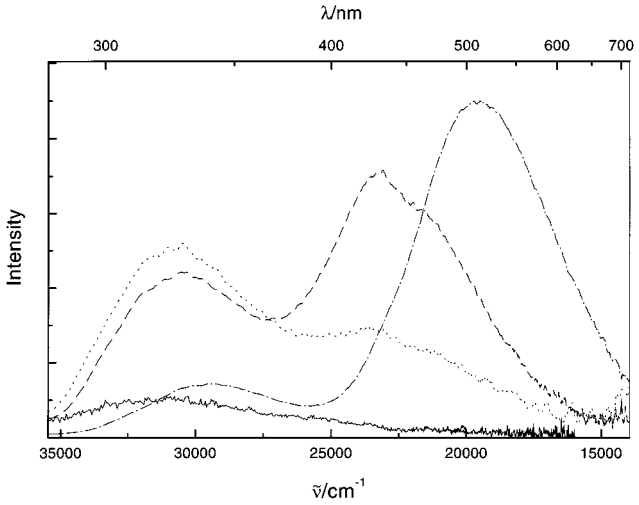

Figure 6. Comparison of the room temperature emission spectra of DMA (— · —), NMA (· · ·), and NCA (- - -) in acetonitrile, and adenosine (—) in water. Please observe that the intensities in this figure are arbitrarily scaled.

TABLE 5: Spectral Positions and Fluorescence Quantum Yields at Room Temperature for DMA, NMA, and NCA in Acetonitrile, and Ado in Water

substance	$\tilde{\nu}_{FB}$/cm^{-1}	$\tilde{\nu}_{FA}$/cm^{-1}	Φ_{FB}	Φ_{FA}
DMA	29500	19600	2.0×10^{-4}	1.5×10^{-3}
NMA	30900	23500	7.9×10^{-5}	5.1×10^{-5}
NCA	30600	23100	1.3×10^{-4}	2.5×10^{-4}
Ado	31900		3×10^{-5}	

A-fluorescence quantum yield follows. However, in the NCA compound, the N^6-methyl of NMA is exchanged for a bulky cyclohexyl substituent which makes the A-state fluorescence of NCA in acetonitrile (Figure 6, Table 5) five times more intense than in NMA while the peak position remains the same. This shows that the A- and B-states of NCA have the same relative energies as in NMA and that the barrier separating the two states is significantly lower, presumably as a consequence of nonplanarity of the cyclohexylamino group in NCA (vide infra).

Thermal Quenching of the B-State. The B-state fluorescence intensity depends strongly on temperature, whereas the A-state fluorescence intensity is almost independent of temperature. The B-fluorescence quantum yield for DM9EA in MTHF increases from 1.6×10^{-4} at 295 K to 0.13 at 80 K. At low temperatures (below the glass temperature) phosphorescence is also observed. This thermal quenching is general for all of the adenine derivatives studied and it is reasonable to assume that a common nonradiative process for all derivatives is responsible for the deactivation of the B-state. First we consider each compound separately and later in the discussion section, a model describing the photophysics for all adenine derivatives will be presented.

In Figure 7, the B-fluorescence quantum yield for DM9EA in EPA[42] is plotted vs temperature. For the moment, the temperature dependence of the B-fluorescence quantum yield (Φ_{FB}) is described by a simple model in which one temperature-dependent and one temperature-independent nonradiative process are considered. This gives

$$\Phi_{FB} = \frac{k_{FB}}{k_{FB} + k_{nr}^0 + k_{nr}(T)} \qquad (3)$$

where k_{FB} is the radiative rate constant for fluorescence from

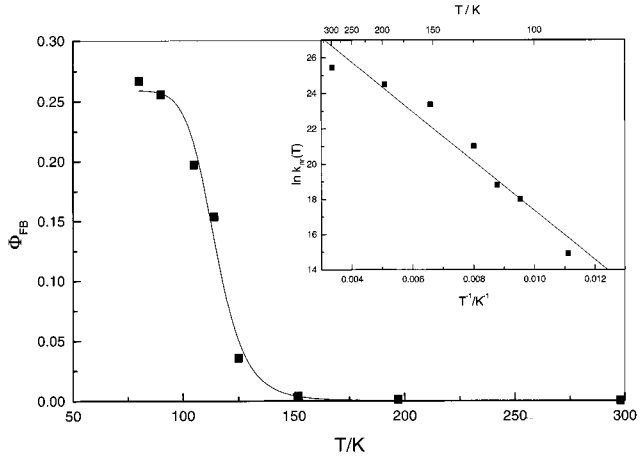

Figure 7. Temperature dependence of the fluorescence quantum yield for DM9EA in EPA.[42] Inset: The Arrhenius plot of the rate constant for nonradiative decay vs inverse temperature.

TABLE 6: Activation Energies for the Nonradiative Deactivation Process of the B-state and Low-Temperature Emission Yields from Measurements in EPA[42]

substance	E_a (kcal/mol)	Φ_F (80 K)	Φ_P (80 K)
DM9EA	2.5	0.27	0.35
NMA	2.1	0.05	0.02
Ado	1.3	0.005	0.01

the B-state, k_{nr}^0 is the rate constant for the temperature-independent nonradiative processes, potentially including both intersystem crossing and internal conversion, and $k_{nr}(T)$ is the rate constant for the temperature-dependent quenching. We further assume that $k_{nr}(T)$ is given by an Arrhenius expression [$k_{nr}(T) = A \exp(-E_a/RT)$] which allows us to evaluate the activation energy, E_a, from the straight line

$$\ln k_{nr}(T) = \ln\left\{\left(\frac{1}{\Phi_{FB}} - 1 - \frac{k_{nr}^0}{k_{FB}}\right)k_{FB}\right\} = \ln A - \frac{E_a}{R}\cdot\frac{1}{T} \quad (4)$$

In Figure 7 the plot ln $k_{nr}(T)$ vs $1/T$ for DM9EA in EPA is inserted. From this and similar plots for NMA and Ado the activation energies for the thermal quenching of the B-fluorescence are found. These are given in Table 6 together with the values of the fluorescence and phosphorescence quantum yields at 80 K.

Discussion

Excited vs Ground State Heterogeneity. When discussing the origin for the A-state fluorescence it is important to exclude the possibility for ground state heterogeneity caused by, e.g., impurities or minor tautomeric forms. This is particularly difficult when the emission quantum yields are small. We have decided to perform a sensitive test by which the excitation spectra of a dilute sample of DM9EA for the two different emissions are compared in cyclohexane where the absorption spectrum is structured (Figure 3). The two normalized excitation spectra overlap entirely, and this clearly shows that both emissions originate from the same primary absorption. Both spectra are also similar in shape to the absorption spectrum, but not identical. This is probably due to imperfect correction of the lamp intensity and/or lack of spectrometer calibration. It should be noted that no fluorescence could be detected with excitation at wavelengths longer than 300 nm and also that the onset of the A-state fluorescence is at wavelengths longer than 400 nm. This large Stokes shift shows that the A-state is structurally and electronically very different from the ground and B-states.

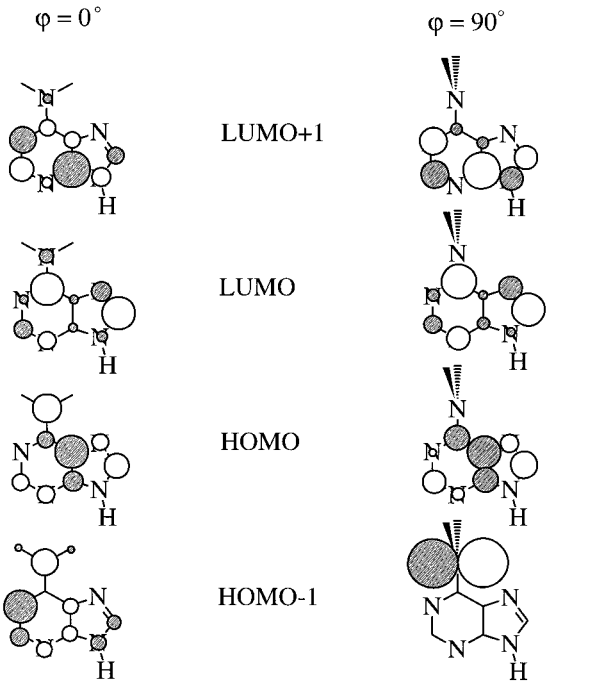

Figure 8. Frontier molecular orbitals calculated (INDO/S) for DMAde in the planar ($\varphi = 0°$) and twisted ($\varphi = 90°$) conformations.

TABLE 7: The Lowest Singlet Electronic Transitions Calculated for DMAde in the Planar ($\varphi = 0°$) and Twisted ($\varphi = 90°$) Conformations Using the INDO/S Method with CI Including All Singly Excited Configurations Formed from the 15 Highest Occupied and 15 Lowest Unoccupied Molecular Orbitals

	transition	$\tilde{\nu}$/cm^{-1}	f^a	dominant configurations
$\varphi = 0°$	$S_0 \rightarrow S_1$ ($\pi\pi^*$)	34 900	0.33	H → L, H → L+1
	$S_0 \rightarrow S_2$ ($\pi\pi^*$)	37 300	0.23	H → L, H → L+1
	$S_0 \rightarrow S_3$ ($n\pi^*$)	39 200	0.001	H-2 → L
$\varphi = 90°$	$S_0 \rightarrow S_1$ ($\sigma\pi^*$)	32 300	0.0003	H-1 → L (CT)
	$S_0 \rightarrow S_2$ ($\pi\pi^*$)	36 400	0.22	H → L
	$S_0 \rightarrow S_3$ ($n\pi^*$)	38 900	0.004	H −3 → L
	$S_0 \rightarrow S_4$ ($\pi\pi^*$)	40 700	0.25	H → L, H → L+1

[a] Oscillator strength.

The A- and B-States of the Adenine Chromophore. We do not have direct experimental evidence for the geometry of the excited states, but the following discussion will show that all present data for DM9EA are consistent with a CT character of the A-state, possibly in combination with structural relaxation along the $-NR_2$ twisting coordinate, i.e., the twisted intramolecular charge transfer (TICT) model by Grabowski and coworkers.[19]

Quantum chemical calculations (INDO/S) show that the lowest excited states of N^6,N^6-dimethyladenine(9*H*) (DMAde) are dominated by configurations involving the two lowest unoccupied (LUMO, L and LUMO+1, L+1) and two highest occupied (HOMO, H and HOMO-1, H-1) molecular orbitals. These orbitals are shown in Figure 8 for the two extreme geometries along the twisting coordinate. In the planar geometry ($\varphi = 0°$) all four orbitals have π-symmetry, but for the twisted geometry ($\varphi = 90°$) the H-1 orbital, which is located on the dimethylamino group, has σ-symmetry with respect to the purine plane. Table 7 shows the energies and dominant configurations for the lowest singlet transitions in the planar and twisted geometries. Upon twisting, the H, L, and L+1 orbitals are

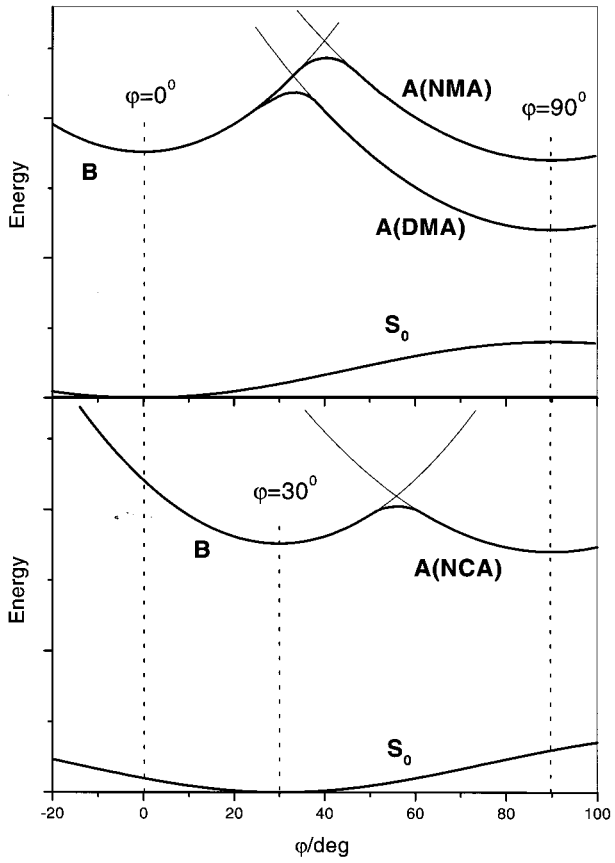

Figure 9. Schematic potential energy surfaces for DMA, NMA, and NCA.

essentially unaffected while the H-1 orbital completely changes character into a σ-symmetric orbital localized on the dimethylamino group. This opens up the possibility for low-energy CT states and, in fact, the lowest transition for the 90° twisted DMAde is a weak CT transition dominated by the H-1→L ($\sigma\pi^*$) configuration (Table 7). The energy of this CT transition is calculated to be much higher than the energy observed for the A-state emission due to omission of the solvent relaxation effects in the calculation. These are expected to be large for a state that differs significantly in polarity from the ground state. As has been mentioned before, the dominance of the CT configuration is also seen in the permanent dipole moment of the A-state which is directed along the N−C_6 axis and almost perpendicular to the ground- and B-state dipole moments.

Figure 9 shows schematic potential energy surfaces for DMA, NMA, and NCA as a function of the −NRR′ twist coordinate (φ). The diabatic B- and A-state potential surfaces are shown as thin lines. The adiabatic states are shown as thick lines, and configurational mixing between the A- and B-states for intermediate twisting angles produces a barrier separating the two states with minima at 90° and 0°, respectively. This is the TICT model applied to the dual fluorescence observed for the N-alkylated adenine derivatives. It should be noted, however, that any other relaxation coordinate that stabilizes the CT state would be an equally likely reaction coordinate. The simplified picture presented in Figure 9 will be used to discuss the kinetics and temperature dependence, and the twisting coordinate could be replaced according to individual preferences as long as it causes the appropriate stabilization of the CT state.

Nonradiative Decay − Temperature Dependence. A very efficient nonradiative process limits the quantum yield of fluorescence for all adenine derivatives studied. In an earlier publication that treated only DMA, we suggested that the photophysical properties could be understood by considering potential energy surfaces such as those in Figure 9, with the addition of a triplet formation channel contributing only at low temperatures.[18] In this model, DMA (or any of the other N-alkylated adenine derivatives) is primarily excited to a Franck−Condon state that is similar to the B-state. Rapid relaxation into the B-state follows, and fluorescence from this state is efficiently quenched by the intramolecular reaction leading to the A-state at room temperature. The fluorescence from the A-state corresponds to a weakly allowed transition ($k_{FA} \approx 10^6$ s^{-1}), and nonradiative processes limit its quantum yield. The intramolecular reaction was suggested to be related to the twisting motion of the dimethylamino group and showed significant temperature dependence. Thus, at lower temperatures the B-fluorescence quantum yield increased while the A-fluorescence was almost constant. At temperatures below 130 K no A-fluorescence could be detected and triplet formation was contributing to the quenching of the B-state.[18]

SCHEME 1

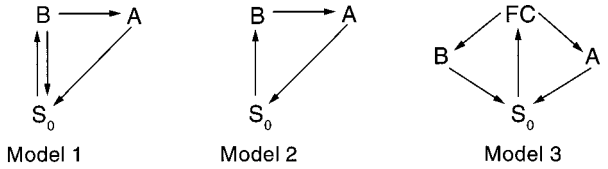

Now, upon removing one of the *N*-methyls the expected blueshift and decrease of intensity of the A-fluorescence occur. However, raising the energy of the A-state, keeping the B-state energy unchanged, we expect a higher barrier between the B- and A-states (compare NMA and DMA in Figure 9) and, thus, a higher activation energy for the nonradiative decay from the B-state. The opposite is observed: In NMA the B-fluorescence quantum yield is lower than in DMA at room temperature (Table 5) and the activation energy for nonradiative decay is slightly smaller (Table 6). This is in direct contradiction to the model suggested for DMA in which nonradiative relaxation of the B-state occurs *through* the A-state. In adenosine, no A-fluorescence at all is detected, presumably because the CT transition is too high in energy, but the B-fluorescence quantum yield and the activation energy for nonradiative decay are even smaller than in the monoalkylated derivatives.

The Photophysics of the Adenine Chromophore. In this section, a model is suggested that describes the photophysical properties of the adenine chromophore and is valid for all compounds presented in this paper. Three different models with increasing complexity will be discussed to make our arguments clear. These models are (Scheme 1) (1) direct internal conversion B→S_0 competing with the formation of the A-state, (2) quenching via the A-state, i.e., B→A→S_0, and (3) the B- and A-states decay independently but share a common parent Franck−Condon state, i.e., S_0←B←FC→A→S_0.

Model 1 is capable of explaining why the quantum yield for fluorescence from the B-state increases as the temperature decreases, and the nonradiative decay can be assigned an activation energy. Since in this model the formation of the A-state competes with the direct internal conversion, an increase in the A-state fluorescence would be expected as the temperature is lowered. This was not observed for DMA earlier and has not been observed for any of the other alkylated adenine derivatives. On the contrary, the A-fluorescence quantum yield is almost constant in the region 295−130 K. This could happen only if the formation of the A-state has the same temperature dependence as the nonradiative decay of the B-state. This led us to suggest model 2 for the photophysics of DMA.[18]

In model 2, the formation of the A-state is the primary

deactivation channel for the B-state and the A-state acts as a bottleneck for return to the ground state. Since the A-state has a lifetime in aprotic solvents of about 1−2 ns, this model implies that ground state recovery would be slow in comparison to what has earlier been suggested for different adenine derivatives.[16] This might in turn have important consequences for the photochemistry of the adenine chromophore.

However, when comparing DMA with NMA (and Ado) we would, from model 2, expect a less efficient quenching of the B-state in the latter compound (vide supra). Since we observe the opposite trend, model 2 has to be discarded. Instead, model 3 is suggested in which the A- and B-states share a common Franck−Condon (FC) state (Scheme 1). This primarily excited state is too short-lived to yield any observable fluorescence. The A- and B-states are formed rapidly from the common FC state and they become "decoupled" in the sense that they could not interconvert. This has the effect that the two states decay independently, and there is not a mother-daughter relationship between them. In Table 4, where the fluorescence lifetime results are reported, it could be noted that all preexponential factors are positive regardless of the emission wavelength. This is a result in favor of model 3 since if the A-state would have been born from the B-state, the preexponential factors would have been negative (rise time) for emission wavelengths corresponding to the A-fluorescence.

The fractions of excited molecules that decay into the A- and B-state is determined by the relative energy of these states and the FC state (more precisely by the location of the potential surface crossings between the FC state and the A- and B-states). This explains why fewer molecules populate the A-state in NMA compared to DMA (and even fewer in Ado); the higher CT state energy in NMA decreases the rate of A-state formation. In the sterically encumbered NCA molecule the alkylamino group is twisted in the ground state (30° according to AM1 calculations). Thus the vertical FC state is distorted in the direction of the A-state potential surface (Figure 9), and the expected increase in A-state population is indeed observed (Figure 6, Table 5).

The thermally activated nonradiative decay of the B-state might still be related to the A-state, but we have at this point no clear evidence for such a relationship. Others have suggested the proximity of $n\pi^*$ states and a corresponding pseudo Jahn−Teller distortion of the lowest excited state as a possible mechanism for nonradiative decay in adenine derivatives and other *N*-heterocycles.[43−45] This mechanism requires the molecule to be distorted along a nontotally symmetric (i.e., out-of-plane) coordinate. Twisting the exocyclic amino group is certainly a nontotally symmetric distortion, and a relation between motion into the CT state and nonradiative decay of the B-state is a conceivable deactivation pathway. We plan to undertake multiconfigurational optimizations of the lowest excited states and seek conical intersections or avoided crossings with the ground state in order to resolve this issue.

Acknowledgment. This work was supported by the Natural Science Research Council (NFR) of Sweden and the Carl Tryggers foundation.

References and Notes

(1) Eisinger, J.; Lamola, A. A. In *Excited States of Proteins and Nucleic Acids*; Steiner, R. F., Weinryb, I., Eds; Macmillan: New York, 1971; p 107.

(2) Callis, P. R. *Annu. Rev. Phys. Chem.* **1983**, *34*, 329.

(3) Cadet, J.; Vigny, P. In *Bioorganic Photochemistry*; Morrison, H., Ed.; John Wiley & Sons: New York, 1990; Vol. 1, p 1.

(4) Ruzsicska, B. P.; Lemaire, D. G. E. In *CRC Handbook of Organic Photochemistry and Photobiology*; Horspool, W. M., Song, P.-S., Eds.; CRC Press: Boca Raton, Florida, 1995; p 1289.

(5) Bujalowski, W.; Graeser, E.; McLaughlin, L. W.; Porschke, D. *Biochemistry* **1986**, *25*, 6365.

(6) Cantor, C. R.; Tao, T. *Procedures in Nucleic Acid Research*; Harper & Row: New York, 1971; Vol. 2.

(7) Longworth, J. W.; Rahn, R. O.; Shulman, R. G. *J. Chem. Phys.* **1966**, *45*, 2930.

(8) Ballini, J. P.; Vigny, P.; Daniels, M. *Biophys. Chem.* **1983**, *18*, 61.

(9) Ballini, J. P.; Daniels, M.; Vigny, P. *Eur. Biophys. J.* **1988**, *16*, 131.

(10) Riegler, R.; Claesens, F.; Kristensen, O. *Anal. Instrum.* **1985**, *14*, 525.

(11) Georghiou, S.; Nordlund, T. M.; Saim, A. M. *Photochem. Photobiol.* **1985**, *41*, 209.

(12) Vigny, P.; Favre, A. *Photochem. Photobiol.* **1974**, *20*, 345.

(13) Vigny, P. Duquesne, M. In *Excited States of Biological Molecules*; Birks, J. B., Ed.; Wiley: New York, 1976; p 167.

(14) Vigny, P.; Ballini, J. P. In *Excited States in Organic Chemistry and Biochemistry*; Pullman, B., Goldblum, N., Eds.; Reidel: Dodrecht, Holland, 1977; p 1.

(15) Wilson, R W.; Callis, P. R. *Photochem. Photobiol.* **1980**, *31*, 323.

(16) Nikogosyan, D. N.; Angelov, D.; Soep, D.; Lindqvist, L. *Chem. Phys. Lett.* **1996**, *252*, 322.

(17) Oraevsky, A. A.; Sharkov, A. V.; Nikogosyan, D. N. *Chem. Phys. Lett.* **1981**, *83*, 276.

(18) Albinsson, B. *J. Am. Chem. Soc.* **1997**, *119*, 6369.

(19) Rotkiewicz, K.; Grellmann, K. H.; Grabowski, Z. R. *Chem. Phys. Lett.* **1973**, *19*, 315.

(20) Rettig, W. *Angew. Chem., Int. Ed. Engl.* **1986**, *25*, 971.

(21) Bhattacharyya, K.; Chowdhury, M. *Chem. Rev.* **1993**, *93*, 507.

(22) Herbich, J.; Grabowski, Z. R.; Wójtowicz, H.; Golankiewicz, K. *J. Phys. Chem.* **1989**, *93*, 3439.

(23) Herbich, J.; Salgado, F. P.; Rettschnick, R. P. H.; Grabowski, Z. R.; Wójtowicz, H. *J. Phys. Chem.* **1991**, *95*, 3491.

(24) Herbich, J.; Karpiuk, J.; Grabowski, Z. R.; Tamai, N.; Yoshihara, K. *J. Luminesc.* **1992**, *54*, 165.

(25) Herbich, J.; Waluk, J. *Chem. Phys.* **1994**, *188*, 247.

(26) Hedayatullah, M. *J. Heterocyclic Chem.* **1982**, *19*, 249.

(27) Berlman, I. *Handbook of Fluorescence Spectra of Aromatic Molecules*; Academic Press: New York, 1965.

(28) This set up is described in detail in Löfroth, J. E., Ph.D. Thesis, University of Göteborg, 1982.

(29) Globals Unlimited, revision 3; Beechem, J. M.; Gratton, E.; Mantulin, W. W.; The Laboratory of Fluorescence Dynamics: University of Illinois at Urbana-Champaign, 1992.

(30) *HyperChem*, version 5; Hypercube, Inc.: Waterloo, Canada, 1994.

(31) *Gaussian 94*, revision B.2; Frisch, M. J.; Trucks, G. W.; Schlegel, H. B.; Gill, P. M. W.; Johnson, B. G.; Robb, M. A.; Cheeseman, J. R.; Keith, T.; Petersson, G. A.; Montgomery, J. A.; Raghavachari, K.; Al-Laham, M. A.; Zakrzewski, V. G.; Ortiz, J. V.; Foresman, J. B.; Cioslowski, J.; Stefanov, B. B.; Nanayakkara, A.; Challacombe, M.; Peng, C. Y.; Ayala, P. Y.; Chen, W.; Wong, M. W.; Andres, J. L.; Replogle, E. S.; Gomperts, R.; Martin, R. L.; Fox, D. J.; Binkley, J. S.; Defrees, D. J.; Baker, J.; Stewart, J. P.; Head-Gordon, M.; Gonzalez, C.; Pople, J. A., Gaussian, Inc.: Pittsburgh, PA, 1995.

(32) The quenching of the long wavelength emission by protic solvents was shown to be dynamic for DMA in ref 18. All adenine derivatives studied so far show this quenching behavior.

(33) Onsager, L. *J. Am. Chem. Soc.* **1936**, *58*, 1486.

(34) Lippert, E. *Z. Naturforsch.* **1955**, *10a*, 541.

(35) Mataga, N.; Kubota, T. *Molecular Intercations and Electronic Spectra*; Marcel Dekker: New York, 1970; p 385.

(36) Bilot, L.; Kawski, A. *Z. Naturforsch.* **1962**, *11a*, 541.

(37) Liptay, W. *Z. Naturforsch.* **1965**, *20a*, 1441.

(38) Lakowicz, J. R. *Principles of Fluorescence Spectroscopy*; Plenum Press: New York, 1983.

(39) Grabowski, Z. R.; Rotkiewicz, K.; Siemiarczuk, A.; Cowley, D. J.; Baumann, W. *Nouv. J. Chim.* **1979**, *3*, 443.

(40) Rettig, W.; Bonacic-Koutecký, V. *Chem. Phys. Lett.* **1979**, *62*, 115.

(41) Staley, R. H.; Taagepera, M.; Henderson, W. G.; Koppel, I.; Beauchamp, J. L.; Taft, R. W. *J. Am. Chem. Soc.* **1977**, *99*, 326.

(42) Solvent mixture 5:5:2 of diethyl ether, 2-methylbutane, and ethanol that forms a clear glass at 80 K.

(43) Lim, E. C. *J. Phys. Chem.* **1986**, *90*, 6770.

(44) Madej, S. L.; Okajima, S.; Lim, E. C. *J. Chem. Phys.* **1976**, *65*, 1219.

(45) Lai, T, Lim, E. C. *Chem. Phys. Lett.* **1979**, *62*, 507.

(46) Bergmann, E. D.; Weiler-Weichenfeld, H.; Neiman, Z. *J. Chem. Soc.* **1970**, B 1334.

(47) Karelson, M. M.; Zerner, M. C. *Int. J. Quantum Chem.* **1986**, *20*, 521.